Phase diagrams of monomer and uv-cured difunctional-acrylate–nematic-liquid-crystal systems

Frédérick Roussel,[1,*] Ulrich Maschke,[2] Jean-Marc Buisine,[1] Xavier Coqueret,[2] and Mustapha Benmouna[1,†]
[1]*Laboratoire de Thermophysique de la Matière Condensée, Equipe de l'UPRESA CNRS 8024, Université du Littoral Côte d'Opale, MREID, F-59140 Dunkerque, France*
[2]*Laboratoire de Chimie Macromoléculaire, UPRESA CNRS 8009, Université des Sciences et Technologies de Lille, F-59655 Villeneuve d'Ascq Cedex, France*

(Received 5 June 2001; revised manuscript received 3 August 2001; published 18 December 2001)

This paper deals with the thermal properties of systems made of the difunctional monomer 1,6-hexanedioldiacrylate (HDDA) and the low-molecular-weight liquid crystal E7. Experimental phase diagrams of uv-cured and uncured solutions of HDDA/E7 systems are established with a polarized optical microscope and a differential scanning calorimeter and the data analyzed within a theoretical formalism that combines the Flory-Huggins model of isotropic mixing and the Maier-Saupe model of nematic order. Ultraviolet-curing samples with a difunctional monomer such as HDDA leads to a crosslinked polymer network and consequently an elastic contribution to the free energy is introduced according to the Flory-Rehner theory of rubber elasticity. The amount of liquid crystal segregated is evaluated to assess the efficiency of the phase separation mechanism.

DOI: 10.1103/PhysRevE.65.011706 PACS number(s): 61.30.−v, 64.70.Md, 64.75.+g, 42.70.Df

I. INTRODUCTION

Molecular compounds showing ordered structures are the subject of intensive investigations both from a fundamental and an applied point of view [1–3]. An important class of these compounds are known as polymer dispersed liquid crystals (PDLCs) and consists of micron sized droplets dispersed in a solid, more or less flexible, polymer matrix [4–6]. These systems have potential applications in areas of high technology such as display devices and privacy windows. Most applications are based on the peculiar electro-optical response behavior of these systems, which, under standard conditions, can be switched from an opaque to a transparent state when a sufficient electric field is applied. Various physical properties are involved in this response such as optical, dielectric, and phase characteristics. Understanding the correlation between those characteristics and the electro-optical (EO) response behavior of PDLCs is the subject of important studies in the literature and among the main topics of discussion in international meetings [7,8]. It is a real challenge to establish precisely the correlation between fundamental properties of PDLC compounds and their performance in practical applications. In a recent study, we have investigated the phase diagrams and the morphology of PDLCs based on nematic-liquid-crystal–monofunctional-acrylate mixtures [9]. The present work goes along these lines but focuses more on establishing the phase diagram of 1,6-hexanedioldiacrylate (HDDA)/E7 mixtures considering both the case of monomer (uncured) and polymer (uv cured) systems. HDDA is a difunctional monomer characterized by a high transparency and a low viscosity and offers favorable conditions for film processing using the uv-curing technique [10–14]. Exposure of HDDA/E7 solutions to uv radiation in the presence of a small amount of photoinitiator produces liquid-crystal (LC) domains dispersed in a crosslinked polymer network with remarkable mechanical, optical, and dielectric properties suitable for EO applications. The low-molecular-weight liquid crystal E7 is an eutectic mixture known for its high birefringence and the wide range of temperature where it shows a nematic order. In spite of the fact that it is a mixture of four paraphenylene derivatives, it presents the advantage of having a single nematic-isotropic (N-I) transition at 61 °C and no other transitions down to −62 °C where it shows a glass transition [15]. Complications related with phase separation among its components in the presence of polymer have been reported in few cases. In particular, peculiar observations were made on various systems such as poly(n-butylacrylate)/E7 [16], Norland 65/E7 [17], and poly(dimethylsiloxane)/E7 [18], which are attributed to preferential adsorption of certain components of E7 on the polymer. Further investigation along these lines are being pursued in our laboratory but it is quite clear to us that these complications are not encountered here. In this paper, we explore the phase behavior of uv-cured and uncured systems in the range from −100 °C to 100 °C. The phase diagrams of these systems are established using a polarized optical microscope (POM) and a differential scanning calorimeter (DSC) and the data analyzed within a formalism combining the Flory-Huggins [19] and Flory-Rehner [20] theories of isotropic mixing and the Maier-Saupe [21] theory of nematic order. The correlation between experimental data and theoretical formalism requires adjustable parameters that are chosen in a way to reach a compromise between a best data fit and a reasonable representation of the systems under consideration. In the next section, we describe the theoretical model while in Sec. III, we give some experimental considerations and in Sec. IV, we discuss the results.

*Author to whom correspondence should be addressed. Email address: Frederick.Roussel@purple.univ-littoral.fr
†Present address: Laboratoire de Recherche sur les Macromolécules, Faculté des Sciences, Université Aboubakr Belkaïd Bel Horizon, 13000 Tlemcen, Algeria.

II. THEORETICAL FORMALISM

A. The isotropic free energy model

For the problem under consideration, the free energy density f is the sum of two terms, one describes the isotropic state $f^{(i)}$ and the second represents the nematic order $f^{(n)}$,

$$f = f^{(i)} + f^{(n)}. \tag{2.1}$$

According to the Flory-Huggins lattice theory [19], which is used for the monomer HDDA system, the isotropic free energy density is given by

$$\frac{f^{(i)}}{k_B T} = \frac{\varphi_1}{N_1}\ln \varphi_1 + \frac{\varphi_2}{N_2}\ln \varphi_2 + \chi \varphi_1 \varphi_2, \tag{2.2}$$

where k_B is the Boltzmann constant, T the absolute temperature, φ_1 and φ_2 are the volume fractions of E7 and HDDA, respectively; $N_1 = 1$ assuming that the LC has a single repeat unit and N_2 is the number of repeat units of HDDA; the interaction parameter χ depends on temperature following the form

$$\chi = A + \frac{B}{T}, \tag{2.3}$$

A and B are numerical constants independent of temperature and composition.

In the case of uv-cured samples, the polymer matrix is a crosslinked network and Eq. (2.2) should be modified accordingly. Using the rubber elasticity theory of Flory-Rehner [20], one has

$$\frac{f^{(i)}}{k_B T} = \frac{3\alpha \varphi_r^{2/3}}{2N_c}(\varphi_2^{1/3} - \varphi_2) + \frac{\beta \varphi_2}{N_c}\ln \varphi_2 + \frac{\varphi_1}{N_1}\ln \varphi_1 + \chi \varphi_1 \varphi_2, \tag{2.4}$$

where N_c is the mean number of repeat units between consecutive crosslinks, φ_r is the initial monomer volume fraction at crosslinking. Polymerization/crosslinking under uv-curing takes place *in situ* meaning that $\varphi_r = \varphi_2$. The rubber elasticity parameters α and β are model dependent. To improve the fit in analyzing data for the present system, we will allow these quantities to depend on the functionality f of monomers at crosslinks and the volume fraction φ_2.

Assuming incompressibility, one has

$$\varphi_1 = \frac{n_1 N_1}{n_0} = 1 - \varphi_2, \tag{2.5}$$

n_0 is the total number of sites in the lattice. For convenience and without loss of generality, we let the reference volume of a unit cell in the lattice to be 1.

To calculate the coexistence curve in regions where two phases are in equilibrium, we solve the following set of equations for the chemical potentials:

$$\mu_1^{\alpha} = \mu_1^{\beta}, \quad \mu_2^{\alpha} = \mu_2^{\beta}, \tag{2.6}$$

where we designate the two phases by the superscripts α and β. The spinodal equation is simply $\partial^2 f / \partial \varphi_2^2 = 0$. Generally, it exhibits two branches separated by the transition line $\varphi_{NI} = T/T_{NI}$ where φ_{NI} is the threshold LC volume fraction below which there is no nematic order. For φ_1 less than φ_{NI}, one recovers the isotropic spinodal branch.

B. The nematic order

The nematic order is described using the Maier-Saupe [21] free energy model

$$\frac{f^{(n)}}{k_B T} = \frac{\varphi_1}{N_1}\left[-\ln Z + \frac{1}{2}\nu \varphi_1 S^2 \right], \tag{2.7}$$

where S is an order parameter, Z the partition function, and ν is known as the Maier-Saupe quadrupole interaction parameter [1,21]. It is proportional to the ratio T_{NI}/T

$$\nu = 4.54\frac{T_{NI}}{T}. \tag{2.8}$$

The orientation order parameter S is defined by

$$S = \frac{1}{2}[3\langle \cos^2 \theta \rangle - 1], \tag{2.9}$$

where θ is the angle between a reference axis and the direction of LC molecules, the symbol $\langle \cdots \rangle$ denotes an average with respect to the equilibrium distribution function $f(\theta)$

$$f(\theta) = \frac{e^{-\dfrac{U(\theta)}{k_B T}}}{Z}. \tag{2.10}$$

The potential $U(\theta)$ is proportional to the zero order Legendre polynomial and to m, a mean field parameter that is a measure of the strength of nematic interaction

$$U(\theta) = -\frac{m}{2}[3\cos^2 \theta - 1]. \tag{2.11}$$

Minimizing the free energy with respect to the order parameter yields

$$m = \varphi_1 \nu S. \tag{2.12}$$

Combining these results, it is easy to show that the nematic contributions to the chemical potentials are [22–25]

$$\frac{\mu_1^{(n)}}{k_B T} = -\ln Z + \frac{\nu \varphi_1^2 S^2}{2}, \tag{2.13}$$

$$\frac{\mu_2^{(n)}}{k_B T} = \frac{1}{2}\frac{N_2}{N_1}\nu \varphi_1^2 S^2. \tag{2.14}$$

Likewise, the spinodal equation requires the second derivative of the free energy

$$\left(\frac{\partial^2 f^{(n)}}{\partial \varphi_1^2}\right)_T = -\frac{1}{N_1}\frac{\partial \ln Z}{\partial \varphi_1}, \tag{2.15}$$

or more explicitly

$$\left(\frac{\partial^2 f^{(n)}}{\partial \varphi_1^2}\right)_T = -\frac{\nu S}{N_1}\left[S+\varphi_1\frac{\partial S}{\partial \varphi_1}\right]. \tag{2.16}$$

III. EXPERIMENT

The monomer HDDA was purchased from UCB Chemicals (Drogenbos, Belgium) and used without purification. HDDA presents a crystalline to isotropic transition at $T_{CrI}=0.2\,^{\circ}\mathrm{C}$ with an enthalpy change of $\Delta H_{NI}=139\ \mathrm{J\,g^{-1}}$. The LC purchased from Merck-Clévenot (Sainte Geneviève des Bois, France) is the eutectic mixture E7 exhibiting a glass transition at $T_g=-62\,^{\circ}\mathrm{C}$ and a nematic to isotropic transition at $T_{NI}=61\,^{\circ}\mathrm{C}$ with $\Delta H_{NI}=4.4\ \mathrm{J\,g^{-1}}$. HDDA/E7 mixtures were prepared with various LC contents and stirred mechanically until they became homogeneous. The polymerization process was induced by 2 weight percent (wt%) of Darocur 1173 (Ciba, Rueil Malmaison, France) with respect to the amount of monomer used. The uv curing was performed using a Seiko-UV 1 unit. The wavelength of the uv radiation was set at $\lambda=365$ nm with a beam intensity of $17.5\ \mathrm{mW\,cm^{-2}}$. The uv-exposure time was fixed at 3 min. Samples for calorimetric measurements were prepared by introducing approximately 3 mg of the initial mixture into aluminum DSC pans, which have been sealed to avoid evaporation effects during the temperature treatment. Samples for microscopy observations were prepared by placing one drop of the reactive mixture between standard glass slides.

The polarized optical microscope (POM) measurements were performed on a Leica DMRXP microscope equipped with a heating/cooling stage Chaixmeca. Samples were first heated from room temperature to a temperature located 15 °C above the isotropic phase limit then quenched at $100\,^{\circ}\mathrm{C\,min^{-1}}$ to $-80\,^{\circ}\mathrm{C}$ for the uncured mixtures and to 20 °C for the cured mixtures. Subsequently another heating cycle with a rate of $5\,^{\circ}\mathrm{C\,min^{-1}}$ up to the isotropic state was carried out. The whole procedure was repeated twice. For both uncured and cured mixtures, two independent samples of the same composition were analyzed.

DSC measurements were performed on a Seiko DSC 220C calorimeter. The DSC cell was purged with $50\ \mathrm{ml\,min^{-1}}$ of nitrogen. Rates of $10\,^{\circ}\mathrm{C\,min^{-1}}$ (heating) and $30\,^{\circ}\mathrm{C\,min^{-1}}$ (cooling) were used in the temperature range -100 to $+100\,^{\circ}\mathrm{C}$. The program consists first in cooling the sample followed by several heating and cooling cycles. Data analysis have been carried out on the second heating ramp.

These methods of sample preparation and experimental procedures for recording DSC thermograms or making POM observations were adopted for several polymer/LC systems [9,26–29]. They are based upon the polymerization induced phase separation method using either uv or EB radiations. The beam intensity, the time of exposure, and the concentration of photoinitiator in the uv case can be chosen to adjust the rate of polymerization/crosslinking and crosslinking density. In all cases the kinetics of phase separation is slower than the kinetics of polymerization/crosslinking in such a way that the LC remains trapped within the polymer network. The amount of LC segregated from the polymer and forming droplets dispersed in the polymer matrix depends upon temperature and composition. One of the aims of this study is to evaluate this amount. Even systems that are characterized by much higher degree of incompatibility (e.g., poly(dimethylsiloxane)/E7 [18], propoxylated glyceroltriacrylate/E7 [30]), and which tend to phase separation much more quickly, exhibit LC droplets dispersed in the polymer matrix under similar conditions of film preparation. It is worthwhile to note that the methods of sample preparation used in this work are quite different from those adopted in Refs. [31–34]. Therefore, the properties of the obtained materials are not expected to follow similar trends.

IV. RESULTS AND DISCUSSION

A. Uncured samples

The knowledge of the phase behavior of prepolymer/LC systems is crucial for the preparation of PDLC films. It defines the thermodynamic stability of the starting mixture via variations of the interaction parameter as a function of composition and temperature. Moreover, the variation of this parameter during the process of polymerization/crosslinking controls to a large extend the morphology and the electro-optical properties of the obtained PDLC films [35–37]. The phase behavior of monomer HDDA/E7 mixtures has been partially investigated in Ref. [38] and briefly discussed in Ref. [8] but only a limited range of temperature has been considered. Here, we cover a wide range of temperature to illustrate the complexity and yet the richness of the phase behavior of this system. For example, Fig. 1 gives the experimental phase diagram of the uncured system as obtained by POM and DSC techniques. Four distinct regions are found. A wide isotropic phase in the upper left-hand side of the diagram. This region covers a large area expressing the extend of miscibility of the two constituents in the mixture. On the right-hand side, as the LC concentration increases, a miscibility gap of the type $(N+I)$ emerges and widens showing a LC phase in the nematic order coexisting with a monomer rich phase in the isotropic state. The nematic phase consists of birefringent spherical droplets dispersed in the monomer isotropic rich phase (black background) as shown in Fig. 2 (top). Through crossed polarizers, the nematic drops exhibit a radial/twisted radial structure, indicating that the LC molecules adopt a homeotropic anchoring at the monomer/LC interface [39]. In principle, a single nematic phase should appear in the vicinity of $\varphi_{LC}=1$ with a trace amount of monomer but this phase was not observed under the present conditions. In the lower part of the diagram as the system is cooled down from the isotropic region, the monomer crystallizes and forms a phase that coexists with an isotropic LC phase [Fig. 2 (middle)]. If a system at composition $0.2\leqslant\varphi_2\leqslant0.4$ is cooled down from the $(N+I)$ region, a similar crystallization phenomenon occurs leading to coexisting

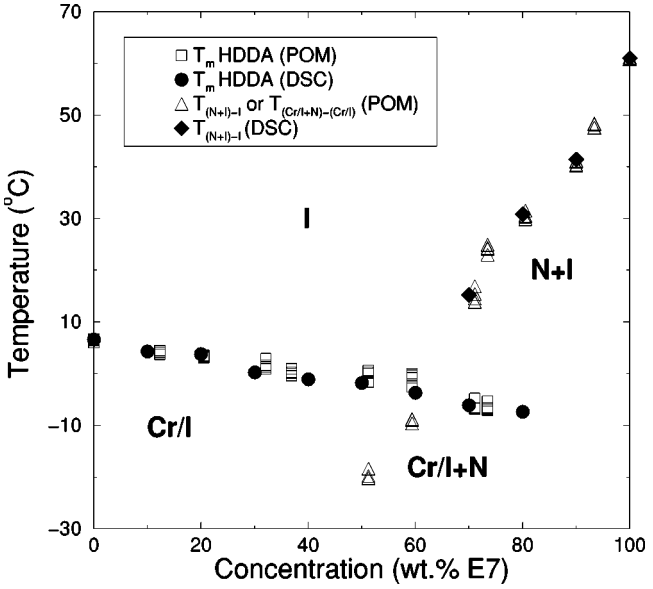

FIG. 1. Experimental phase diagram of the monomer HDDA/E7 system as obtained by POM and DSC spectra in an extended range of temperature. Four distinct regions are observed: isotropic (I), nematic + isotropic ($N+I$), crystalline/isotropic (Cr/I), and crystalline/isotropic + nematic (Cr/$I+N$). T_m is the melting temperature of HDDA (Cr$\rightarrow I$).

phases with a dispersion of crystallites as shown in Fig. 2 (bottom): the monomer rich phase hosts the crystallites and the nematic LC rich phase consists of spherical droplets. Both POM and DSC data corroborate these splitting transitions and yield consistent results.

Figure 3 shows the DSC thermal spectra for the same system with compositions ranging from zero (pure HDDA monomer) to 100 wt% (pure E7) with 10% increment. It gives the transitions existing in the temperature range from $-105\,^{\circ}$C to $95\,^{\circ}$C. The bottom curve corresponding to pure E7 exhibits a glass transition at $T_{gE7}=-62\,^{\circ}$C and a nematic to isotropic transition at $T_{NI}=61\,^{\circ}$C. By adding monomeric HDDA, both transitions are shifted to lower temperatures. From 20 wt% HDDA, a second glass transition is observed at $T_{gHDDA}=-96\,^{\circ}$C corresponding to a supercooled isotropic monomer rich phase, which recrystallizes then melts upon heating. The melting peak widens and shifts to higher temperatures when HDDA concentration increases. For pure HDDA, the melting transition T_m is found near $0\,^{\circ}$C. The T_g and $N\rightarrow I$ transitions are shown by small kinks while the recrystallization and melting transitions correspond to relatively large peaks indicating substantial energy transfers. Variations of these energy transfers with the composition will be analyzed below in the case of uv-cured samples.

B. Ultraviolet-cured systems

Figure 4 gives the DSC thermograms of uv-cured HDDA/E7 system covering the whole range of composition from pure HDDA to pure E7. A wide range of temperature extending from -90 to $+100\,^{\circ}$C is explored. Remarkable differences are found compared to the uncured systems involving HDDA monomer. The number of DSC peaks is significantly reduced, and the thermograms show no evidence of recrystallization or melting transitions due to the uv-curing. The $N\rightarrow I$ transition temperature of the phase separated LC is close to that of pure E7, i.e., $T_{NI}\sim 61\,^{\circ}$C. The glass transition temperature of the LC domains also remains nearly constant, i.e., around $T_{gE7}\sim -62\,^{\circ}$C. These results clearly indicate that the phase separated LC domains are rather pure or at least behave as pure E7. However, this does not imply that the LC forms a single macrophase completely separated from the polymer network. It simply means that one has domains in the form of droplets containing oriented LC molecules. These features are obtained from a combina-

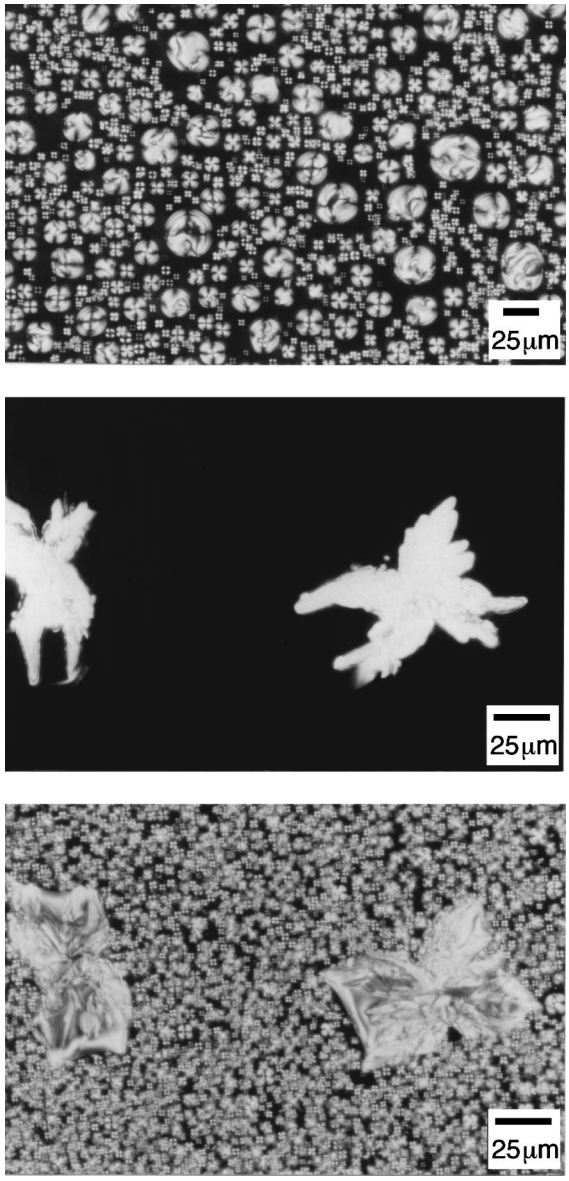

FIG. 2. Optical microphotographs showing the texture of monomeric HDDA/E7 mixtures: top, ($N+I$) region at $T=5\,^{\circ}$C and $\varphi_2=18$ wt% (crossed polarizers mode, $P\perp A$, magnification 200×); middle, (Cr/I) region at $T=-9\,^{\circ}$C and $\varphi_2=40$ wt% (crossed polarizers mode, $P\perp A$, magnification 320×); bottom, (Cr/$I+N$) region at $T=-25\,^{\circ}$C and $\varphi_2=40$ wt% (crossed polarizers mode, $P\perp A$, magnification 320×).

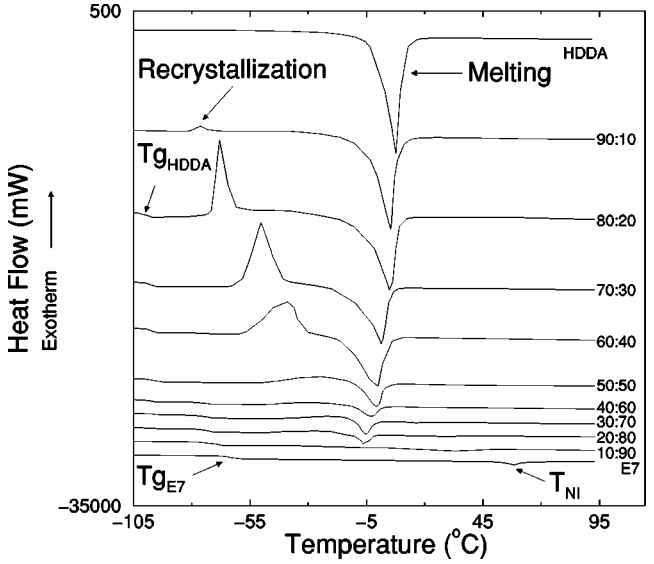

FIG. 3. DSC spectra (heating rate $10\,^{\circ}\mathrm{C\,min^{-1}}$) of the monomeric HDDA/E7 system for several compositions and in an extended temperature range as indicated on this figure. T_{gHDDA} and T_{gE7} are the glass transition temperatures of the supercooled monomer and the LC, respectively, and T_{NI} is the nematic to isotropic tansition temperature of E7.

tion of thermograms and POM observations and help establish the phase diagram as shown in Fig. 5. Obviously uv-cured and uncured HDDA/E7 systems exhibit completely different phase properties. While both diagrams show a single isotropic phase and a two phases ($N+I$) region, uv-cured samples are characterized by a miscibility gap of the type ($I+I$) even at high temperatures. This is typical of the phase behavior of crosslinked polymers where elastic forces

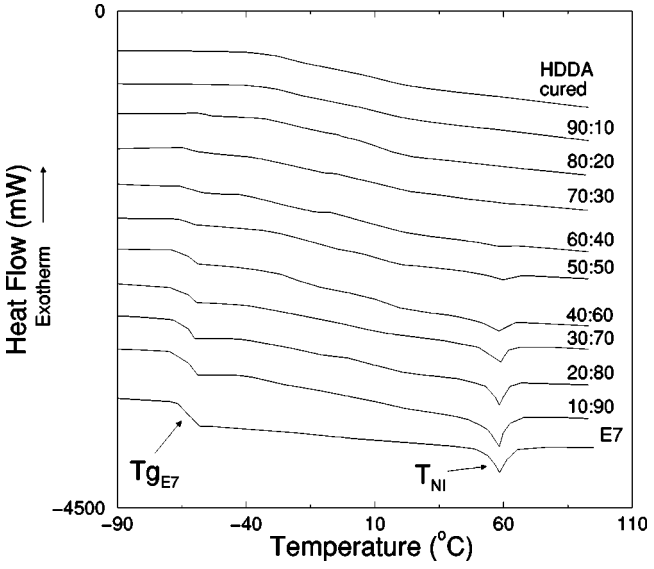

FIG. 4. Thermograms obtained from DSC measurements (heating rate $10\,^{\circ}\mathrm{C\,min^{-1}}$) for a series of uv-cured HDDA/E7 mixtures for LC concentrations ranging from 0 to 100 wt %. T_{gE7} is the glass transition temperature of the LC, and T_{NI} is the nematic to isotropic tansition temperature.

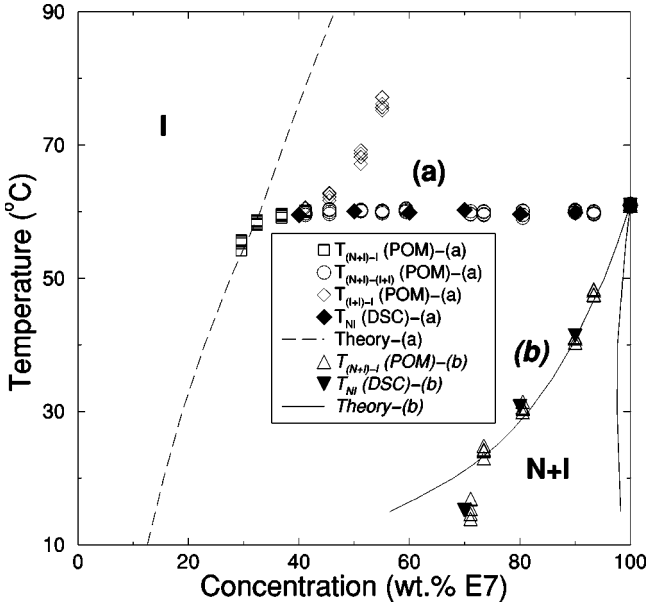

FIG. 5. Equilibrium phase diagrams of HDDA/E7 systems obtained from POM and DSC techniques. The upper part (a) corresponds to the uv-cured system (plain text legend), while the lower part (b) is for the monomer system (italic legend). T_{NI} and $T_{(N+I)-I}$ represent the transition temperature of the phase separated liquid crystal between the nematic and isotropic states, $T_{(N+I)-(I+I)}$ is the (nematic+isotropic) to (isotropic+isotropic) transition temperature, and $T_{(I+I)-I}$ is the (isotropic+isotropic) to isotropic transition temperature. The solid (uncured) and dashed (uv-cured) lines are theoretical calculations made using (a) $N_1=1$, $N_c=5$, $\chi=-1.6+823/T$, $\alpha=\{[f-2(1-\varphi_2)]/f\}$, $\beta=[(2\varphi_2)/f]$, and $f=3$ [40]; (b) $N_1=1$, $N_2=2$, and $\chi=-1.88+887/T$. In both cases, we have used $T_{NI}=61\,^{\circ}\mathrm{C}$.

at the cross links oppose polymer stretching beyond the saturation limit. At this limit, any additional amount of LC forms an excess pure LC macrophase in contrast with linear polymers and monomers where the LC phase is in principle never entirely pure. Figure 6 shows optical micrographs of uv-cured HDDA/E7 (18:82) samples at $T=45\,^{\circ}\mathrm{C}$ using the crossed polarizer mode (bottom), and $T=65\,^{\circ}\mathrm{C}$ where the polarizer (P) and the analyzer (A) were oriented parallel to each other (top). The nematic + isotropic ($N+I$) phase is characterized by a large number of small birefringent microdroplets as shown in Fig. 6 (bottom). This micrograph gives the clear evidence that LC droplets are dispersed in the polymer network and do not form a single macrophase completely separated from the polymer film. Figure 6 (top) corresponds to the isotropic miscibility gap ($I+I$). The close refractive indices of the two isotropic phases combined to the high density and the small size of the LC domains lead to a relatively low contrast. This is the major difficulty of observation of the ($I+I$) morphology, especially in the LC concentration range $0.3\leqslant\varphi_1\leqslant0.45$. However, it should be noted that the ($I+I$) domain of the uv-cured HDDA/E7 system covers a wide range of temperature and concentration. Calculation of the binodal curve (Fig. 5, dashed line) is made using a mean number of repeat units between crosslinks

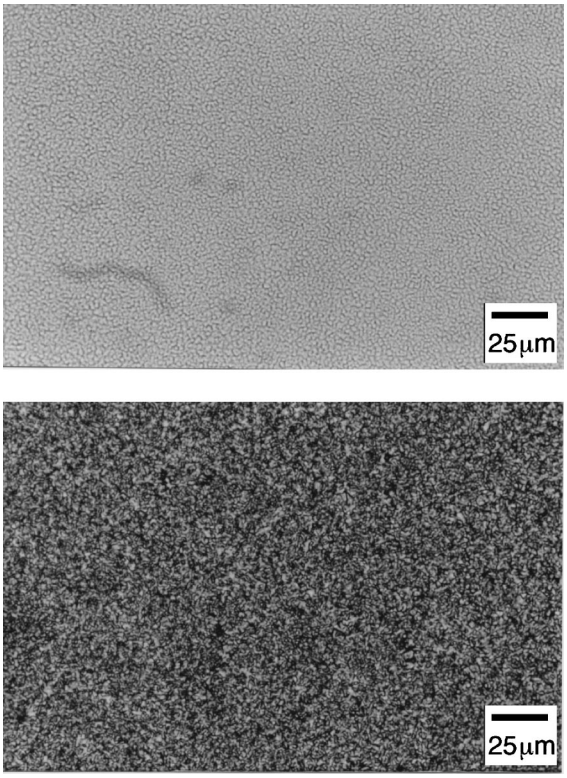

FIG. 6. Optical microphotographs showing the texture of a uv-cured HDDA/E7 mixture: top, $(I+I)$ region at $T=65\,^{\circ}\mathrm{C}$ and $\varphi_2=18$ wt% (parallel polarizers mode, $P\|A$, magnification 320×); bottom, $(N+I)$ region at $T=45\,^{\circ}\mathrm{C}$ and $\varphi_2=18$ wt% (crossed polarizers mode, $P\perp A$, magnification 320×).

$N_c=5$, which is a reasonable value for a polymer network prepared with a difunctional monomer like HDDA.

The theoretical analysis of the phase diagram of the monomer system in the upper temperature range has been reported elsewhere [8]. We give it here for the sake of comparison and completeness. The lower part displays the diagram in a temperature range where the monomer does not exhibit a crystalline structure. Note the consistency between experimental data (symbols) and the calculated curve (solid line). Neither the spinodal curve nor the critical point appear in this figure because they lie outside the (T,φ_1) domain considered here. The agreement between experiments and theory is reached with a reasonable choice of parameters. However, the single nematic phase predicted by the calculations on the right-hand side for the uncured system is not observed experimentally because this observation is at the edge of accuracy of the techniques used here (i.e., POM and DSC).

Figure 7 shows the variations of ΔH_{NI} and ΔC_p vs $\varphi_1=\varphi_{LC}$ for monomer and uv-cured HDDA/E7 systems. ΔC_p and ΔH_{NI} are inferred from the heat capacity change at T_g and from the enthalpy change at the $N\rightarrow I$ transition, respectively. Both quantities (ΔH_{NI} and ΔC_p) increase linearly with the LC concentration φ_{LC} and are nearly parallel. When the monomer crystallizes, the solubility of E7 is sharply reduced. The variation of ΔH_{NI} vs φ_{LC} for the monomer system is linear and lies below that of the cured sample espe-

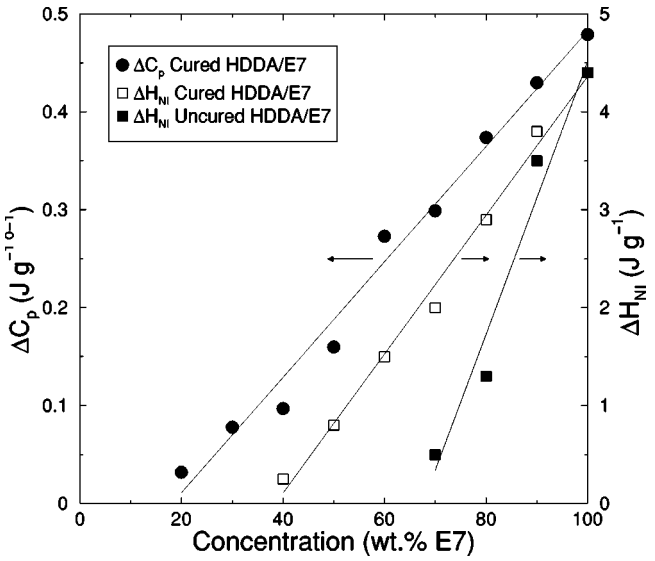

FIG. 7. Variation of the enthalpy ΔH_{NI} at the $N\rightarrow I$ transition (right y axis) and the heat capacity ΔC_p at T_g (left y axis) vs $\varphi_{LC}=\varphi_1$. Both monomer and uv-cured systems are represented for comparison.

cially at low LC compositions, showing the increased miscibility of the monomer and the LC before polymerization. In order to estimate quantitatively these results, the LC solubility limit η has been determined by linear regression of the experimental data sets, followed by calculating the x axis intercepts. In the case of the monomer HDDA/E7 mixtures, the value of η was 68%, whereas in the case of polymerized samples, a value of 38% was found. For the cured system, the value of η extracted from ΔC_p ($\eta=18\%$) is lower than from ΔH_{NI} ($\eta=38\%$). This can be explained by the fact that the solubility of LC molecules in the polymer network at the glass transition temperature $T_{gE7}\sim-62\,^{\circ}\mathrm{C}$ is lower than that at the nematic-isotropic transition temperature $T_{NI}\sim 61\,^{\circ}\mathrm{C}$ [41,26].

Figure 8 shows the variation of γ, the amount of LC segregated in the nematic droplets as a function of φ_{LC}. This is a central quantity in the thermodynamic analysis of PDLC systems and is a measure of the efficiency of the phase separation mechanism. The upper curve corresponds to the uv-cured HDDA/E7 system at $T_{gE7}\sim-62\,^{\circ}\mathrm{C}$. It shows that the amount of LC segregated at a low temperature is larger than that at the $N\rightarrow I$ transition. As the LC concentration increases, γ first raises and tends to level off as φ_{LC} approaches 1. This highly nonlinear behavior is consistent with the theoretical prediction of Eq. (4.1) represented by the solid and dashed lines [41–43,27,26]

$$\gamma=\frac{m_1^D}{m_1}=\frac{\delta}{\varphi_1}, \tag{4.1}$$

where m_1^D is the mass of LC in the nematic domain and m_1 is the one in the whole mixture. Letting δ be the ratio of enthalpy changes at the $N\rightarrow I$ transition or heat capacity changes at T_{gE7} for the mixture at composition φ_1 and for the bulk LC,

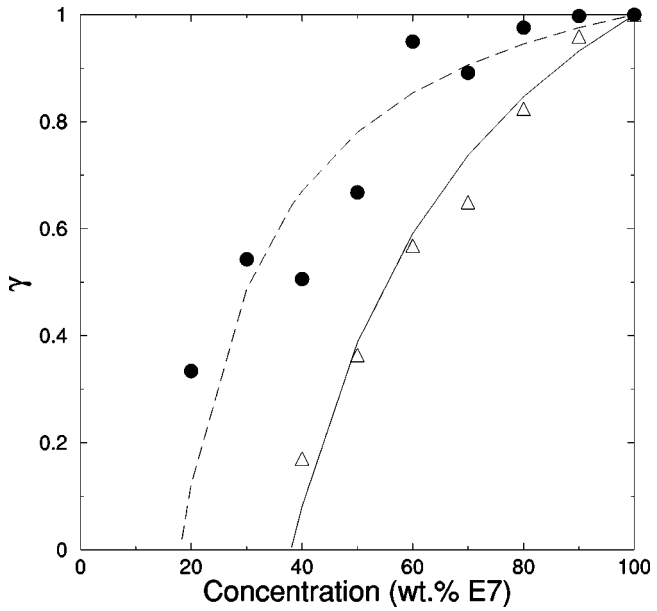

FIG. 8. Variation of γ the amount of segregated LC vs $\varphi_{LC}=\varphi_1$ for the uv-cured HDDA/E7 system. The open diamonds represent γ calculated from Eq. (4.1) using Eq. (4.2) with ΔH_{NI} values, whereas the filled circles were determined using ΔC_p data. The dashed and solid lines are the theoretical predictions of Eq. (4.1) using Eq. (4.3).

$$\delta=\frac{\Delta H_{NI}(\varphi_1)}{\Delta H_{NI}(\varphi_1=1)}=\frac{\Delta C_p(\varphi_1)}{\Delta C_p(\varphi_1=1)}, \tag{4.2}$$

The rule of inverse segments yields a relationship between δ and the solubility limit η as

$$\delta=\frac{(\varphi_1-\eta)}{(1-\eta)}, \tag{4.3}$$

where $\varphi_1>\eta$, otherwise $\delta=0$. These equations assume that the LC inside nematic domains and in the pure state have similar thermal properties and the polymer in the LC phase does not contribute to $\Delta H_{NI}(\varphi_1)$ or $\Delta C_p(\varphi_1)$.

V. CONCLUSION

Ultraviolet-curing mixtures of the difunctional monomer HDDA and E7 lead to PDLC systems with a crosslinked polymer network in which a dispersion of LC droplets takes place. The phase diagrams of those systems and those of analogous monomer/LC mixtures are established by POM and DSC techniques in a range of temperature going from -100 to $+100\,^{\circ}$C. The phase diagram of uncured mixtures exhibits characteristic regions such as crystalline, nematic and isotropic phases due to crystallization of the monomer. For the cured system, an isotropic miscibility gap $(I+I)$ has been clearly evidenced, consistent with the theoretical predictions. The experimental results of both systems were analyzed reasonably well within a simple formalism associating mean field approximations of isotropic mixing, rubber elasticity theory, and nematic ordering. The amount of heat capacity change at the glass transition and of the enthalpy change at the $N\rightarrow I$ transition are found to decrease linearly with decreasing LC concentration. Extrapolation to zero of the heat capacity change and of the enthalpy change yields the solubility limit of the LC in the polymer or monomer substrate, consistent with the phase diagrams in the (T,φ_{LC}) frame. The amount of LC segregated drops suddenly at a certain composition showing a highly nonlinear variation with the composition.

ACKNOWLEDGMENTS

This work has been accomplished during a stay of Mustapha Benmouna at the Université du Littoral Côte d'Opale. The Région Nord-Pas de Calais, the CNRS, the MENRT, and the FEDER are acknowledged for financial support.

[1] P.G. De Gennes and J. Prost, *The Physics of Liquid Crystals*, 2nd ed. (Clarendon Press, Oxford, 1995).
[2] S. Chandrasekhar, *Liquid Crystals*, 2nd ed. (Cambridge University Press, Cambridge, 1992).
[3] *Handbook of Liquid Crystals*, edited by D. Demus, J. Goodby, G.W. Gray, H.-W. Spiess, and V. Vill (Wiley-VCH, Weinheim, 1998).
[4] P.S. Drzaic, *Liquid Crystal Dispersions* (World Scientific, Singapore, 1995).
[5] J.W. Doane, in *Liquid Crystals: Their Applications and Uses*, edited by B. Bahadur (World Scientific, Singapore, 1990).
[6] D.A. Higgins, Adv. Mater. **12**, 251 (2000).
[7] F. Roussel, U. Maschke, J.-M. Buisine, and X. Coqueret, in *Proceedings of the 17th International Liquid Crystal Conference, Strasbourg, France, 1998*, edited by A. Skoulios and D. Guillon (Gordon and Breach Science Publishers, Paris, 1998); Mol. Cryst. Liq. Cryst. Sci. Technol., Sect. A **329**, 199 (1999).
[8] F. Roussel, U. Maschke, J.-M. Buisine, X. Coqueret, and M. Benmouna, Mol. Cryst. Liq. Cryst. Sci. Technol., Sect. A **365**, 685 (2001).
[9] F. Roussel *et al.*, Phys. Rev. E **62**, 2310 (2000).
[10] C.A. Guymon *et al.*, Science **275**, 57 (1997).
[11] B. Nabeth, J.-F. Gerard, and J.-P. Pascault, J. Appl. Polym. Sci. **60**, 2113 (1996).
[12] A. Matsumoto and A. Taniguchi, Polymer **31**, 711 (1999).
[13] J. Masere, F. Stewart, T. Meehan, and J.A. Pojman, Chaos **9**, 315 (1999).
[14] S.W. Kang, S. Sprunt, and L.C. Chien, Appl. Phys. Lett. **76**, 3516 (2000).
[15] Value given by Merck Eurolab, Darmstadt, Germany.
[16] T. Bouchaour *et al.*, Liq. Cryst. **27**, 413 (2000).
[17] P. Nolan, M. Tillin, and D. Coates, Mol. Cryst. Liq. Cryst. Sci. Technol., Sect. A **8**, 129 (1992).
[18] N. Gogibus *et al.*, Eur. Polym. J. **37**, 1079 (2001).

[19] P.J. Flory, *Principles of Polymer Chemistry* (Cornell University Press, Ithaca, 1965).
[20] P.J. Flory and J. Rehner, J. Chem. Phys. **12**, 412 (1944).
[21] W. Maier and A. Saupe, Z. Naturforsch. A **14A**, 882 (1959); *ibid.* **15A**, 287 (1960).
[22] C. Shen and T. Kyu, J. Chem. Phys. **102**, 556 (1995).
[23] F. Brochard, J. Jouffroy, and P. Levinson, J. Phys. (Paris) **45**, 1125 (1984).
[24] F. Benmouna, L. Bedjaoui, U. Maschke, X. Coqueret, and M. Benmouna, Macromol. Theory Simul. **7**, 599 (1998).
[25] F. Benmouna, U. Maschke, X. Coqueret, and M. Benmouna, Macromol. Theory Simul. **9**, 215 (2000).
[26] F. Roussel, J.-M. Buisine, U. Maschke, and X. Coqueret, Mol. Cryst. Liq. Cryst. Sci. Technol., Sect. A **299**, 321 (1997).
[27] U. Maschke, F. Roussel, J.-M. Buisine, and X. Coqueret, J. Therm. Anal. **51**, 737 (1998).
[28] U. Maschke *et al.*, Macromolecules **32**, 8866 (1999).
[29] U. Maschke *et al.*, Macromol. Chem. Phys. **202**, 1100 (2001).
[30] U. Maschke *et al.*, Polym. Bull. **44**, 577 (2000).
[31] V. Vorflusev and S. Kumar, Science **283**, 1903 (1999).
[32] T. Qian, J.-H. Kim, S. Kumar, and P.L. Taylor, Phys. Rev. E **61**, 4007 (2000).
[33] V.V. Krongauz, E.R. Schmelzer, and R.M. Yohannan, Polymer **32**, 1654 (1991).
[34] P.L. Taylor, Y.-K. Yu, and X.Y. Wang, J. Chem. Phys. **105**, 1237 (1996).
[35] C. Serbutoviez, J.G. Kloosterboer, H.M.J. Boots, and F.J. Touwslager, Macromolecules **29**, 7690 (1996).
[36] C. Grand, M.F. Achard, and F. Ardouin, Liq. Cryst. **22**, 287 (1997).
[37] K. Amundson, A. van Blaaderen, and P. Wiltzius, Phys. Rev. E **55**, 1646 (1997).
[38] F. Roussel, Ph.D. thesis, Université du Littoral-Côte d'Opale, Dunkerque, France, 1996.
[39] H.S. Kitzerow, Liq. Cryst. **16**, 1 (1994).
[40] P.J. Flory, J. Chem. Phys. **18**, 108 (1950).
[41] G.W. Smith, G.M. Ventouris, and J.L. West, Mol. Cryst. Liq. Cryst. Sci. Technol., Sect. A **213**, 11 (1992).
[42] G.W. Smith, Mol. Cryst. Liq. Cryst. **180B**, 201 (1990).
[43] G.M. Russell, B.J.A. Paterson, C.T. Imrie, and S.K. Heeks Chem. Mater. **7**, 2185 (1995).